Letamo *et al. Geoenvironmental Disasters* (2023) 10:19
https://doi.org/10.1186/s40677-023-00249-2

Geoenvironmental Disasters

RESEARCH

Open Access

Unified earthquake catalogue and mapping of Gutenberg–Richter parameters for the East African Rift System

Alemayehu Letamo[1*], B. Kavitha[1] and T. P. Tezeswi[1]

Abstract

Background The initial phase of earthquake hazard assessment involves the consolidation of diverse magnitude scales, thereby requiring the homogenization of various magnitudes. Moment magnitude (Mw) emerges as the preferred descriptor for a range of magnitudes, encompassing local magnitude (ML), teleseismic magnitude (e.g., mb and MS), duration magnitudes (MD), and other magnitude proxies. Unlike alternative scales, Mw does not exhibit saturation at high magnitudes, enhancing its reliability. To achieve uniformity in magnitude representation, diverse regression techniques are employed, with the General Orthogonal Regression (GOR) method being widely regarded as the most dependable, accounting for uncertainty in both independent and dependent variables.

Methods This study utilized the International Seismological Centre (ISC) Catalogue (http://www.isc.ac.uk/) to compile an array of events related to the East Africa Rift System (EARS). Subsequently, the General Orthogonal Regression method was applied to merge and harmonize the collected data. Furthermore, the research computed Gutenberg-Richter b-values using the newly unified magnitude.

Results Notably, the conversion relationships between magnitude proxies, including MS-mb, mb-Mw, MS-Mw, and ML-Mw, exhibited robust correlations, with coefficients of 0.86, 0.80, 0.88, and 0.94, respectively. In contrast, the relationship between ML and mb proxies revealed a notably weaker correlation, registering a coefficient of 0.54. Ultimately, the study identified a magnitude of completeness and a b-value of 3.8 and 0.71, respectively, for the EARS region, providing valuable insights for earthquake hazard assessment in this area.

Conclusion Generally, the homogeneous catalogue is a step forward in seismicity assessment and geodynamic activities in the EARS. Hence, developing the empirical equations for the area is essential for future studies on seismic hazards and engineering applications due to the peculiarity of EARS's geological and tectonic characteristics.

Article highlights

- The empirical relations developed on the basis of the updated catalogue for the EARS are crucial and strong agreement with global studies for the earthquake hazard analysis in the region.
- The magnitude of completeness, Mc, for the EARS is significantly low as catalogues are continuously being updated.
- b-value obtained reveals that the EARS is experiencing active stress field with b-value significantly lower than 1.

*Correspondence:
Alemayehu Letamo
letamo@student.nitw.ac.in
Full list of author information is available at the end of the article

Keywords Earthquake, General orthogonal regression, Homogeneous, East African Rift System, b-values

Introduction

The East African Rift System (*EARS*), a roughly 5000 km long continental rift that dates back to the Cenozoic period, extends from the Afar triple junction, which links the horn of Africa with the Middle East, up to western Mozambique. There are ongoing extensions from the Indian Ocean to Botswana and the Democratic Republic of the Congo. Geologists can learn more about how rifts in continents evolve over time into oceanic spreading centres like the Mid-Atlantic Ridge thanks to the fact that it is the only ongoing continental-scale rift system in the world (Fig. 1; Styron and Pagani 2020).

The EARS typically has two branches: the western branch, which is characterized by earthquakes of extensional rifting, and the eastern branch, which is more volcanically active. (e.g., Yang and Chen 2010; Delvaux et al. 2012). The western branch is composed of the *NE–SW* moving Albert-Edward rift, the N–S trending Kivu rift,

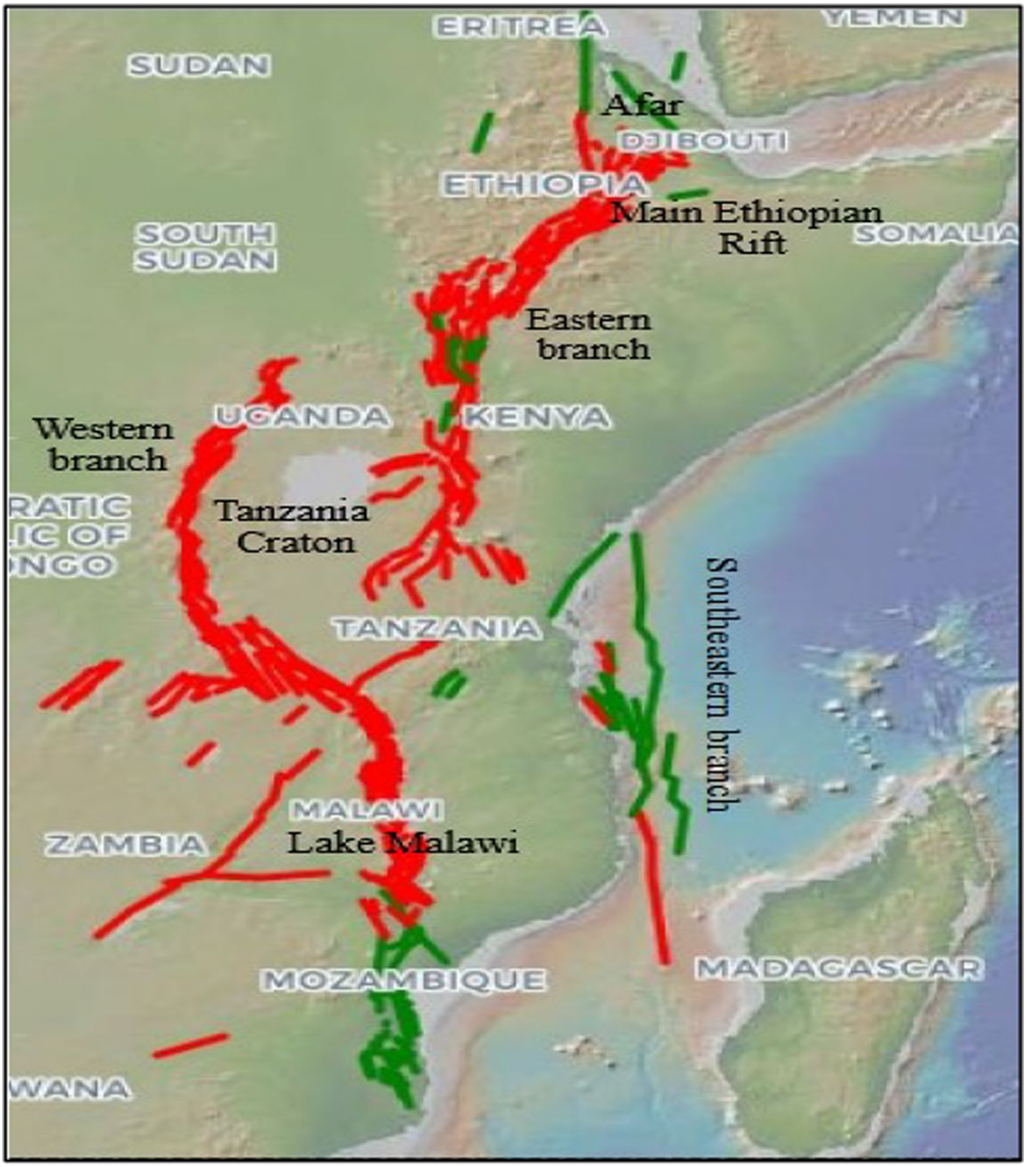

Fig. 1 The EARS with major active faults (adapted from GEM Global Active Faults Database)

and the *NW–SE* trending Tanganyika rift. (Fig. 1; Delvaux et al. 2012). The eastern branch is made up of a collection of rifts that aren't connected to one another, the majority of which have been impacted by magmatism. The eastern flank of *EARS* includes the northern Tanzania divergence, the Ethiopian Rift, the Kenya Rift, and the Davie Ridge, enumerated from north to south. Between the two *EARS* flanks is the Tanzanian craton, which contrasts with neighboring Paleoproterozoic to Neoproterozoic orogenic belts by appearing thicker, colder, and stronger (Delvaux 2001).

Generally speaking, one of the most active continental rift systems with many destructive tremors documented is the EARS in the African continent's most seismically active region, East Africa (Letamo et al. 2023). The Salima Earthquake of Malawi in the 1989 M_w 6.3 (Williams et al. 2022), the 1990 earthquake of M_S 7 and M_S 7.1 of South Sudan (Kebede and Van Eck 1997), the 13 December 1910 M_S 7.4 Rukwa (Tanzania) event (Ambraseys and Adams 1991), the M_w 6.8 event of the Congo in 2005 are salient manifestations of earthquakes in the *EARS*. Numerous people have died as a result of these earthquakes, and the region's poorly built structures have sustained enormous property losses.

The unification of various magnitudes is the first step in the evaluation of earthquake risk. Magnitudes ought to be uniform. Thus, moment magnitude should be used to describe various heterogeneous magnitudes, including local and teleseismic magnitudes (such as m_b and M_S). Moment magnitudes (M_w) do not saturate for big magnitudes, in contrast to local magnitudes (M_L) and teleseismic magnitudes (mb & MS) (Scordilis 2006).

Moment magnitude (M_w) is the standard magnitude measure used to categorize earthquakes according to size. Compared to other magnitude measures, it is more closely associated with the energy of an earthquake.

For global data, researchers have used a variety of regression methods (Scordiliss 2006; Wason et al. 2012; Lolli et al. 2014; Weatheril et al. 2016). Whilst different researchers have developed local magnitude relations for Africa (Eluyemi et al. 2019; Lamesa et al. 2019; Boudebouda et al. 2022).

In general, regressions are normally executed using empirical relations with a Simple Orthogonal Regression (*SOR*) method (Ambraseys 1991) or the Ordinary Least Squares (*OLS*) method, which both presume the same level of ambiguity and the presumption that the independent variable is error-free (Gasperini & Ferrari 2000) in that order. Nonetheless, general orthogonal regression (*GOR*) techniques employ different degrees of biases for the two factors (Castellaro et al. 2006). In recent years, the *GOR* strategy has become more popular among researchers as the most consistent procedure for regressing magnitudes (Castellaro et al. 2006; Wason et al. 2012; Mobarki & Talbi 2022). Standard regression errors could even reach 0.3–0.4, according to Castellaro et al. (2006), considerably distorting estimates of the parameters used in seismic hazard analysis.

Since the region of study is seismically active, falling in the newly forming continent-wide rift system, it is prone to various stress causing forces. In the region forces responsible for the stress could be the boundary forces at the plates' sides and basal tractions at the base of the plate, and gravitational potential energy from density heterogeneities causing crustal stresses and deformations (Medvedev 2016; Rajaonarison et al. 2021). However, the latter is the most influencing factor that drives the seismicity of the EARS owing to the fact that the region is well known for its high elevations (e.g., East African plateaus and southern Africa plateaus; Stamps et al. 2014). Accordingly, all factors triggering the seismicity and the associated hazard occurrences need to be addressed and updated as new data emerge.

For this study, heterogeneous occurrences for the EARS were gathered from the *ISC* catalogue. After that, the data was combined using the General Orthogonal Regression technique. The conclusions are then made using comparisons from both local and international empirical relations.

Methodology

Sources

As a result of its suitability and completeness nature of worldwide data, our study data were collected from *ISC* catalogue in the latitude (25°S − 20°N) and longitude (25°E − 52°E) for the time extent of 1900–2022. A total of 27,000 events with magnitudes ranging from 2.5 to 7.5 with various magnitude scales and depths between 0 and 700 km were recorded in the specified period. After a completeness check, a total of 21,333 events were selected for regression analysis (see Fig. 2). Nevertheless, only 2,568 events, with sufficient numbers of pairs (refer Table 1) were selected to make the relationships between the magnitude proxies of *Mw*. Sometimes the connection can be implicitly inferred from another proxy magnitude when data is lacking.

Magnitude conversion

Unbiased and homogenous earthquake magnitude measure is required in order to evaluate seismic risks caused by different earthquake magnitudes. Most earthquake data is not recorded in moment magnitude (M_w) scale, which is directly derived from the seismic moment (M_0) and represents the amount of energy released. In addition, because the moment magnitude scale is not susceptible to saturation at higher magnitudes, it has additional

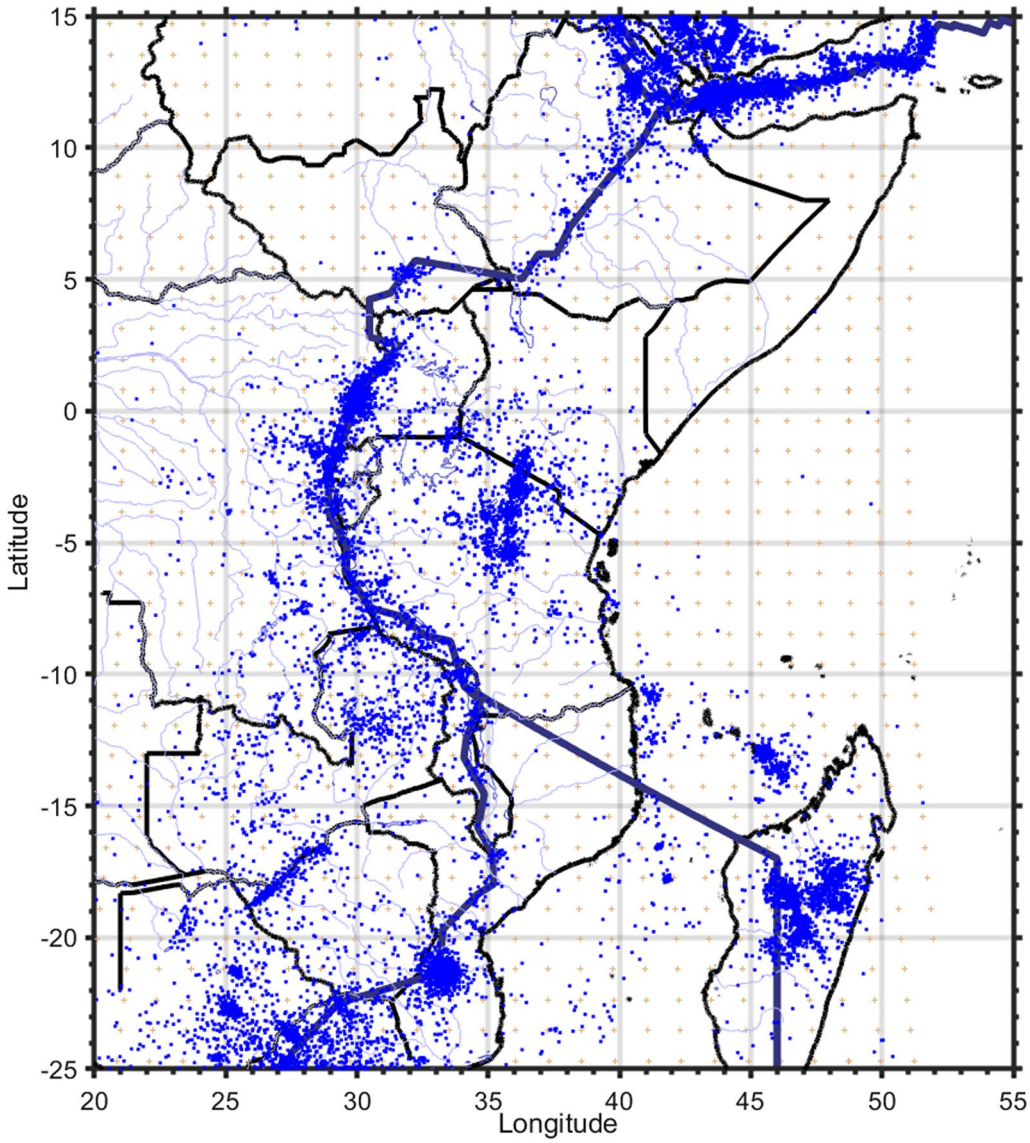

Fig. 2 The seismic events for the EARS from 1900 to 2022: with blue dots showing earthquake events and black lines represent Plate boundaries and borders

Table 1 Number of events used for GOR analysis

Dependent variable	Independent variable	Number of data
M_s	m_b	1649
M_w	m_b	54
M_w	M_s	46
m_b	M_L	280
M_d	M_L	539

benefits over many other earthquake measuring scales (Das et al. 2013). The majority of events are typically quantified in scales of M_L, M_S, m_b etc. There are, of course, very few M_w events that are directly determined from data. In order to accurately identify the earthquake hazard parameters (e.g., M_{min}, b, and M_{max}), conversion from other scales must be established. Table 2 provides a review of worldwide and local relations for the

Table 2 Review of various regression models for different scales

Independent variable	Outcome variable	Regression model	References
m_b	$M_{w.}$	$0.85m_b + 1.03$; $R^2 = 0.86$; $3.5 \leq m_b \leq 6.2$	Scordilis (2006)
$M_{S.}$	$M_{w.}$	$0.67M_S + 2.07$; $R^2 = 0.77$; $3 \leq M_S \leq 6.1$	Scordilis (2006)
$M_{S.}$	M_w	$0.99M_S + 0.08$; $R^2 = 0.81$; $6.2 \leq M_S \leq 8.2$	Scordilis (2006)
$M_{D.}$	$M_{w.}$	$0.764M_D + 1.379$; $3.7 \leq M_D \leq 6.0$	Akkar et al. (2010)
$M_{L.}$	$M_{w.}$	$0.953M_L + 0.422$; $3.9 \leq M_L \leq 6.8$	Akkar et al. (2010)
m_b	$M_{w.}$	$1.084m_b - 0.142$; $R^2 = 0.88$; $m_b < 6.5$	Weatherill et al. (2016)
$M_{S.}$	m_b	$0.703\ M_S + 1.534$;$R^2 = 0.744$	Ibrahim et al. (2015)
m_b	$M_{w.}$	$0.834m_b + 1.181$; $R^2 = 0.99$; $3.1 \leq m_b \leq 6.5$	Lamessa et al. (2019)

conversion of various magnitudes to M_w. In our study, regression analysis was performed using *Statgraphics 19 Centurion* (https://www.statgraphics.com/).

This study employed the General Orthogonal Regression (*GOR*) approach due to its superiority in terms of overall performance. We utilized error ratios between $\lambda = 0.2$ and $\lambda = 7$, as suggested by Castellaro et al. (2006), which falls within the range of $\lambda = 1.25$ and $\lambda = 7$.

Seismicity parameters

In order to assess earthquake hazards, dependent events must first be removed from the catalogue. In order to accomplish this, a window that is defined in both the space and time dimensions must be created, and dependent events (foreshocks and aftershocks) must be eliminated from the updated catalogue. The Gardner and Knopoff's (1974) method is one of the techniques used to window catalogues in space–time window in (Eq. 1):

$$d[\text{km}] = 10.^{0.1238*M_w+0.983}; \quad t[\text{days}] = \left\{ \begin{array}{l} 10.^{0.032*M_w+2.7389}, M_w \geq 6.5 \\ 10.^{0.5409*M_w-0.547}, M_w < 6.5 \end{array} \right\}, \tag{1}$$

In order to accurately predict seismic hazard, the Gutenberg–Richter (*G–R*) *b*-value is a vital variable. The local cut-off point, M_c, must be selected in this way to optimize the *G–R* relation's reliability. The M_c value is also influenced by additional factors, including the number and caliber of the sensors, their geometrical layout, and the level of background noise. The accuracy of the *b*-value calculation determines the effectiveness of the technique. The Maximum Curvature technique (*MAXC*), developed by Wiemer and Wyss (2000), was used in this manuscript to assess the completeness check in the frequency magnitude distribution.

Once the independent events with complete catalogue is defined, the determination of b-values is most crucial and determined by Gutenberg and Richter (1944) relation:

$$\log n(m) = a - bm$$

The frequency-magnitude distribution is described by the constants *a* and *b*, and *n* is the size of population of earthquakes with a magnitude exceeding *m*. The productivity of earthquakes is described by parameter *a*, and the relative size distribution of events are described by parameter b.

The magnitude of b is typically 1 or very close to 1 for seismicity of tectonic origin (Muller & Jokat 2000), and a value of b less than 1 denotes the dominance of larger earthquakes in relation to smaller events. Reduction in the frequency of low-magnitudes earthquakes, particularly in seismically active areas, indicate the build-up of stress, while high seismicity in the area may be explained by high b-values in the volcanic chambers (Sanchez et al. 1995). Low b values suggest that the earth's crust is under significant differential stress, which points to the completion of the Seismic Cycle (Schorlemmer et al. 2005). The Seismic Cycle can be referred as the sequence of repeated stresses, strains, and energy releases in the Earth's crust that cause earthquakes.

The maximum likelihood technique and the least square fit method are used to compute b values, but the assumption that every data point has the same weight and residuals are Gaussian-distributed makes the least square method biased. Aki (1965) proposed the maximum likelihood technique (*MLE*) to circumvent these inconveniences.

In this study, *ZMAP* (Weimer, 2001) was used to determine *GR* parameters, such as *b*-values, *a*-values and *Mc*, using an *MLE* method in log scale.

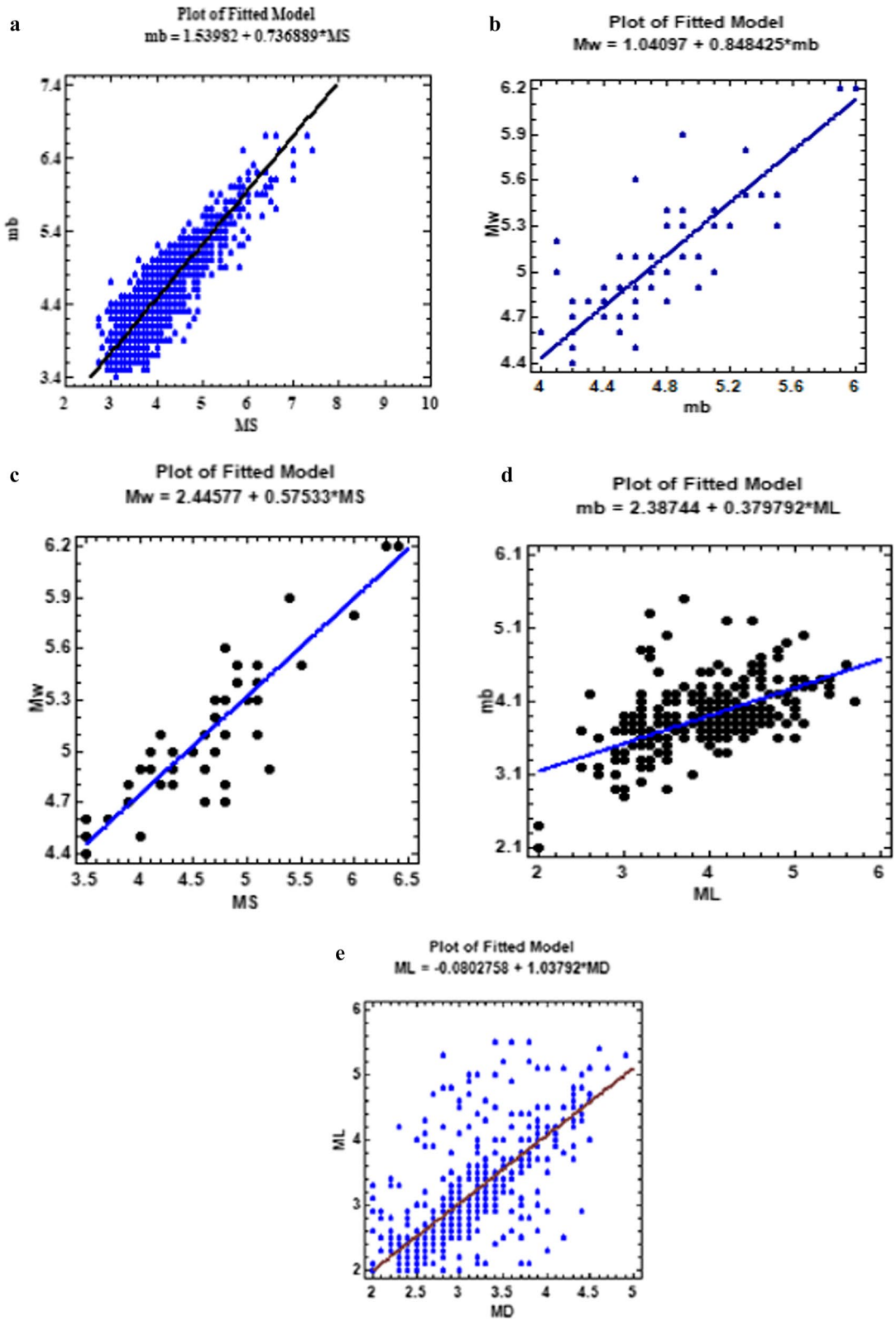

Fig. 3 *GOR* Models for earthquake magnitudes in various scales for *EARS*

Results and discussion

Magnitude conversion

From Eqs. (2)–(7) provide the regression relations developed for different magnitude proxies while Fig. 3 displays the *GOR* findings of this study against various regression models.

We deploy the General Orthogonal Regression relation to compute $m_b - M_w$ pairs (Eq. 2):

$$\begin{aligned} &M_w = 0.848(\pm 0.086)m_b + 1.041(\pm 0.413);\ R^2 = 0.808 \\ &4.0 \le m_b \le 6.0;\ n = 54;\ \lambda = 1.25;\ \zeta = 0.25 \\ &M_w = 1.429(\pm 0.15)m_b - 2.576(\pm 0.22);\ R^2 = 0.64 \\ &6 \le m_b \le 6.7;\ n = 18;\ \lambda = 2.44;\ \zeta = 0.31 \end{aligned} \tag{2}$$

We relate M_S to m_b using relation in Eq. (3):

$$\begin{aligned} mb = 0.72(\pm 0.01)M_S + 1.54(\pm 0.1);\ R.^2 = 0.86 \\ 2.7 \le M_S \le 7.4;\ N = 1649;\ \lambda = 7;\ \zeta = 0.32 \end{aligned} \tag{3}$$

m_b is related to M_L in *GOR* analysis (Eq. 4):

$$\begin{aligned} m_b = 0.381(\pm 0.04)M_L + 2.4(\pm 0.14);\ R.^2 = 0.54 \\ 2.0 \le M_L \le 5.7;\ N = 280;\ \lambda = 7;\ \zeta = 0.38 \end{aligned} \tag{4}$$

Conversion from M_S to M_w in *GOR takes the form in* Eq. (5):

$$\begin{aligned} &0.55(\pm 0.04)M_S + 2.56(\pm 0.2);\ R.^2 = 0.88 \\ &3.5 \le M_S \le 6;\ N = 46;\ \lambda = 7;\ \zeta = 0.2 \\ &0.752(\pm 0.13)M_S + 1.574(\pm 0.09);\ R.^2 = 0.907 \\ &3.5 \le M_S \le 7.4;\ N = 21;\ \lambda = 0.54;\ \zeta = 0.14 \end{aligned} \tag{5}$$

Using *GOR*, as shown in Equation, homogenizes the Duration Magnitude (M_D) into the local magnitude (M_L):

$$\begin{aligned} M_L = 1.041(\pm 0.05)M_D - 0.082(\pm 0.15);\ R.^2 = 0.67 \\ 2.0 \le M_D \le 4.9;\ N = 539;\ \lambda = 7;\ \xi = 0.291 \end{aligned} \tag{6}$$

Moreover, Eq. 6 is used to convert from local magnitude to moment magnitude.

$$\begin{aligned} 0.781(\pm 0.09)M_L + 1.492(\pm 0.32);\ R.^2 = 0.94 \\ 2.1 \le M_L \le 4.1;\ N = 12;\ \lambda = 7;\ \zeta = 0.19 \end{aligned} \tag{7}$$

Comparisons with different studies

We compare our findings with relations from various studies at global scale (e.g., Scordilis 2006; Akkar et al. 2010; Weatherill et al. 2016) and studies around the EARS (Lamessa et al. 2019; Ibrahim et al. 2015). The comparisons are presented for m_b-M_w and M_S-Mw pairs in Fig. 4.

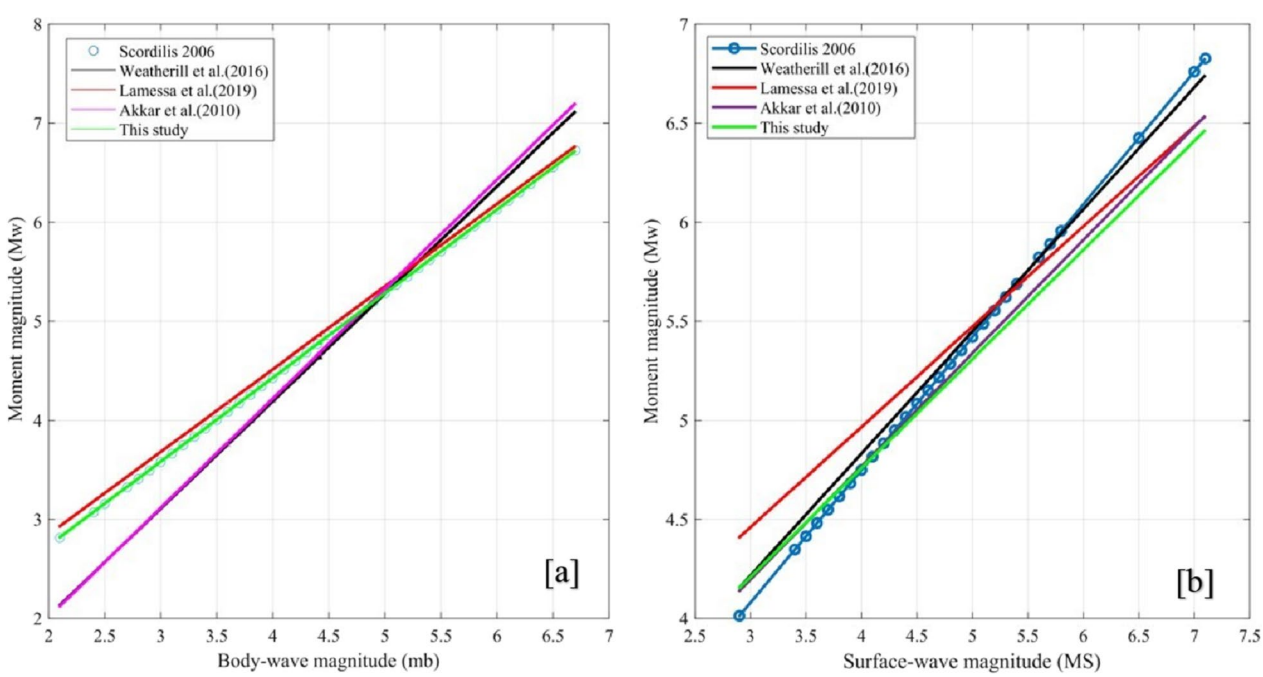

Fig. 4 Comparisons of various global and local empirical relations: **a** m_b-M_w, **b** *Ms-Mw*

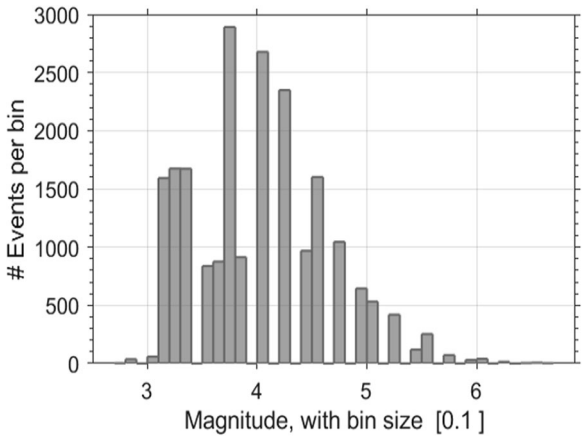

Fig. 5 Number of Events versus magnitude size in a bin size of 0.1

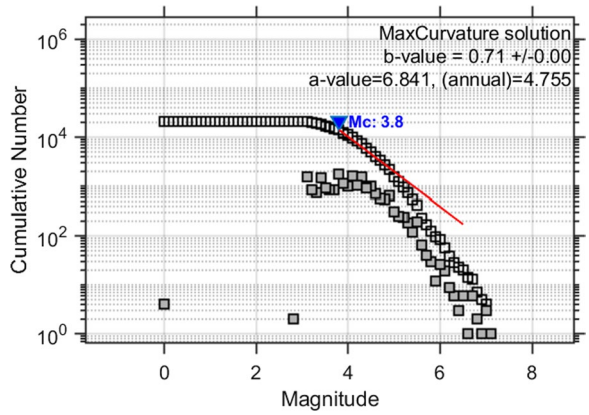

Fig. 8 G-R parameters of the EARS With b-value = 0.71; EARS (1900–2022) Mc = 3.8; a-value for the period (1900–2022) = 6.82

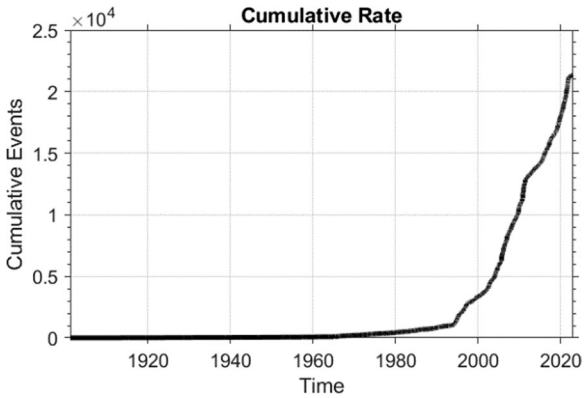

Fig. 6 Temporal variation of the Cumulative Events in the EARS from 1900 to 2022

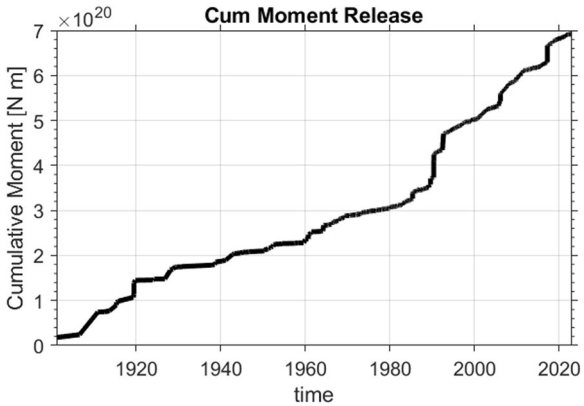

Fig. 7 Cumulative moment release for the

Table 3 *G-R* Parameters of the *EARS* for the time 1900–2022

Region	M_c	*b*	*a-value*
Afar	*4.1*	0.91 ± 0.09	*5.75*
NMER	*4.1*	0.83 ± 0.07	*5.45*
CMER	4.1	0.75 ± 0.08	4.98
SMER	4.9	0.89 ± 0.1	6.16
Tanzanian Craton	4.3	1.29 ± 0.16	7.4
Lake Kivu	3.1	0.52 ± 0.04	3.78
Mozambique	4.9	1.37 ± 0.21	8.4

G–R parameters

Generally the seismicity of the *EARS* is moderate type with some stronger events (see Fig. 5). The temporal variation of events (Fig. 6) and Cumulative Moment release of the *EARS* (Fig. 7) both demonstrate a sharp rise in graph depicting that the recording facilities of the region have only improved late 1990s.

Magnitude of completeness M_c for *EARS* in regional level using the *MLE* method was found to be *3.8* for the entire range of study (*1900–2022*) as shown in Fig. 8. However, the *G-R* parameters varied from place to place and temporally. The *b*-values, M_c and *a*-values of typical parts of the *EARS* such as Afar, northern Main Ethiopian Rift (*NMER*), central Main Ethiopian (*CMER*), Sothern Main Ethiopian Rift (*SMER*), Tanzanian Craton, and Mozambique are presented in Table 3. Most notably, one can deduce that the seismicity of the *EARS* is active with few exceptions such as areas under stable Tanzanian Craton, and some southern Africa parts (e.g., southern Mozambique) exhibit less

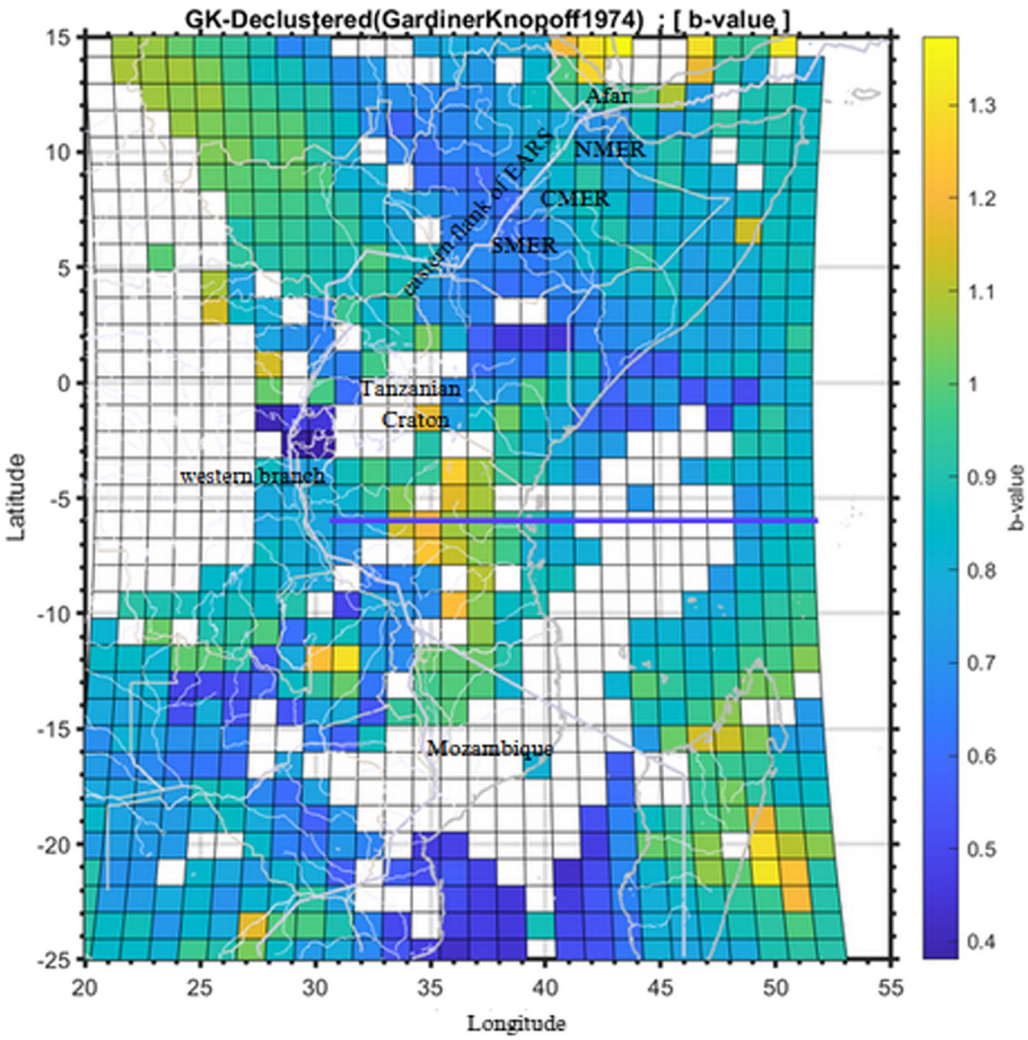

Fig. 9 Spatial distribution of b-values in the *EARS* ranging from Afar, the triple junction of the *EARS*, to Mozambique, in the southern extreme of the rift. Here, grid size of 1.15°×1.15° was used. Moreover, the minimum number of events used per node were 50

seismic activities. Afar triple junction, which links the horn of Africa with the Middle East, up to western Mozambique is a seismically active part where sea-floor spreading is observed. South of Afar triple junction is the main Ethiopian Rift with *b*-values of *0.84 ± 0.08*, *0.75 ± 0.08* and *0.89 ± 0.1* for *NMER*, *CMER*, and *SMER* respectively.

Farther more, Lake Kivu, the western flank of the *EARS* experienced *b*-values relatively lower than in the eastern flank of the *EARS* reaching b-value of ~ 0.5. Western flank is highly active in terms of seismicity as low *b-values* could reveal. This can be attributed to high seismic moment release which has an inverse relation with *b-values* (Dipok et al., 2018). On the contrary, the area between the eastern flank and the western flank of the *EARS* is less seismic with *b*-value of *1.29*. This is the area with underlying thicker and stable Tanzanian Craton. Far towards south is also the stable and less seismic block in the southern Mozambique with *b*-value of 1.37 (*see* Table 3*;* Fig. 9).

Conclusions

For hazard assessment, an earthquake catalogue is a crucial necessity. Therefore, using accurate and bias free homogeneous relation is essential. For sub-Saharan areas like the *EARS*, however, this is not an easy job. Numerous studies are accessible on both a global and local level, but there aren't any regional empirical equations based on recent data. The purpose of this article is to close this gap. We can derive the following conclusions from this paper:

- The development of empirical equation for the area is essential for future studies on seismic hazard and engineering applications due to peculiarity in the geological and tectonic characteristics of *EARS*.
- The global empirical relation obtained by Scordilis (2006) and the m_b-M_w relation from this study strongly agree. However, the *Ms-Mw* relation firmly agrees with the relationship found in Akkar et al., (2010). Figure 3 presents the variations observed between various studies and this study.
- To enhance the seismicity assessment of the *EARS*, the largest active tectonic rift system in the world, empirical relationships between $M_S - m_b, m_b - M_w, M_S - M_w, and M_L - M_w$ magnitude proxies have been investigated. The most trustworthy collection of the *ISC* catalogue data for the period 1900 to 2022 were used. With correlation coefficients of 0.86, 0.80, 0.88, and 0.94, respectively, the conversion of the magnitude proxies $M_S - m_b, m_b - M_w, M_S - M_w, and M_L - M_w$ exhibits strong correlation, whereas the magnitude proxies $M_L - m_b$ relation exhibits comparatively weak correlation. The homogeneous catalogue is a step forward in seismicity assessment programs and geodynamic activities in *EARS*.
- Even though the East Africa Rift Region is much affected by rifting and volcanic eruptions, the predominating seismicity in the region is of tectonic origin as one can infer from the b-value which is lower than 1. This lower value could be attributed to the influence emanating from the gravitational potential energy originated from topography and density contrasts.
- The average depth of the events in the EARS from ISC catalogue (http://www.isc.ac.uk/) is ~ 13.8 km which marks the rift region zone to be a zone of shallow seismicity which could be traced that the *EARS* is likely acting as continental spreading ridge. The data are obtained by simple arithmetic mean of the depth of the events in the region.

Appendix

General orthogonal regression

Let's assume that η and ζ are the true values of independent and dependent variables, respectively, η_t and ζ_t are their observed values. Furthermore, we further assume that η and ζ have measurement errors of ψ and δ as measurement errors, respectively. Therefore, we obtain:

$$\eta = \eta_t + \psi \tag{8}$$

$$\zeta = \zeta_t + \delta, \tag{9}$$

and the regression model is:

$$\zeta = a + b\eta_t + \delta, \tag{10}$$

where b and a are the slope and intercept of linear relationships, respectively.

If, C_η^2, C_ζ^2 and $C_{\eta\zeta}$ are the sample covariance of η,ζ, and between ζ, and η then

$$C_\zeta^2 = \hat{b}^2\hat{\sigma}_{\eta t}^2 + \upsilon\hat{\sigma}_\psi^2 \tag{11}$$

$$C_\eta^2 = \hat{\sigma}_{\eta_t}^2 + \hat{\sigma}_\psi^2, \tag{12}$$

$$C_{\eta\varsigma} = \hat{b}\hat{\sigma}_{\eta t}^2 \tag{13}$$

where the error variance ratio is:

$$\upsilon = \frac{\sigma_\delta^2}{\sigma_\varepsilon^2} \tag{14}$$

Combining the above equations, we arrive at

$$\hat{b} = \frac{C_\zeta^2 - \upsilon C_\eta^2 + \sqrt{\left(C_\zeta^2 - \upsilon C_\eta^2\right)^2 + 4\upsilon C_{\eta\zeta}^2}}{2C_{\eta\zeta}\eta\zeta} \tag{15}$$

Acknowledgements

Authors are grateful to the ISC (http://www.isc.ac.uk/) website for providing invaluable data, without which this study would not have been possible. Additionally, we extend our thanks to ZMAP (Wiemer 2001) from which we greatly benefited the analysis results and presentation graphs. In this study, seismicity data were compiled from the ISC catalog (http://www.isc.ac.uk/), accessed February 2023 GC. In case additional data is needed to support this study, you can contact the corresponding author [Alemayehu Letamo].

Author contributions

AL and BK worked on the design of the study, analysis, and the draft of the article. Whereas, TPT gave critical feedback and shaped the manuscript.

Declarations

Competing interests

The authors declare no competing interests pertaining to this article.

Author details

[1]Department of Civil Engineering, National Institute of Technology Warangal, Telangana 506004, India.

Received: 10 April 2023 Accepted: 30 August 2023
Published online: 06 September 2023

References

Akkar S, Çağnan Z, Yenier E, Erdoğan Ö, Sandikkaya MA, Gülkan P (2010) The recently compiled Turkish strong motion database: Preliminary investigation for seismological parameters. J Seismolog 14(3):457–479. https://doi.org/10.1007/s10950-009-9176-9

Ambraseys NN, Adams RD (1991) Reappraisal of major African earthquakes, south of 20°N, 1900–1930. Nat Hazards 4(4):389–419. https://doi.org/10.1007/BF00126646
Bora DK, Borah K, Mahanta R, Borgohain JM (2018) Seismic b-values and its correlation with seismic moment and Bouguer gravity anomaly over Indo-Burma ranges of northeast India: tectonic implications. Tectonophysics 728–729:130–141. https://doi.org/10.1016/j.tecto.2018.01.001
Boudebouda A, Athmani A, Das R (2022) A unified earthquake catalog for Northern Algeria based on an advanced moment magnitude scale using a robust regression method. ResearchSquare. https://doi.org/10.21203/rs.3.rs-1930439
Castellaro S, Mulargia F, Kagan YY (2006) Regression problems for magnitudes. Geophys J Int 165(3):913–930. https://doi.org/10.1111/j.1365-246X.2006.02955.x
Statgraphics Centurion 19 Software; Manugistics Inc., Rockville (2019)
Chorowicz J (2005) The East African rift system. J Afr Earth Sc 43(1–3):379–410. https://doi.org/10.1016/j.jafrearsci.2005.07.019
Das R, Wason HR, Sharma ML (2013) General orthogonal regression relations between body-wave and moment magnitudes. Seismol Res Lett 84(2):219–224. https://doi.org/10.1785/0220120125
Delvaux D, Kervyn F, Macheyeki AS, Temu EB (2012) Geodynamic significance of the TRM segment in the East African Rift (W-Tanzania): active tectonics and paleostress in the Ufipa plateau and Rukwa basin. J Struct Geol 37:161–180. https://doi.org/10.1016/j.jsg.2012.01.008
Delvaux D (2001) Tectonic and palaeostress evolution of the Tanganyika-Rukwa-Malawi rift segment, East African Rift System. Peri-Tethys Memoir 6: Peri-Tethyan Rift/Wrench Basins and Passive Margins 545–567
Eluyemi AA, Baruah S, Baruah S (2019) Empirical relationships of earthquake magnitude scales and estimation of Guttenberg-Richter parameters in gulf of Guinea region. Sci Afr 6:e00161. https://doi.org/10.1016/j.sciaf.2019.e00161
Gasperini P, Ferrari G (2000)Deriving numerical estimates from descriptive information: the computation of earthquake parameters. In: Annali di Geofisica, vol 43, Issue 4, pp 729–746. https://doi.org/10.4401/ag-3670
Ibrahim KY, Babiker NM, Ali MH, Warage A, Humeda KA (2015) A unified Mw-based earthquake catalog of Sudan and adjacent regions for the period 1408–2014. Am J Earth Sci 2(5):150–156
Kebede F, Van Eck T (1997) Probabilistic seismic hazard assessment for the Horn of Africa based on seismotectonic regionalisation. Tectonophysics 270(3–4):221–237. https://doi.org/10.1016/S0040-1951(96)00215-6
Lamessa G, Mammo T, Raghuvanshi K (2019) Homogenized earthquake catalog and b-value mapping for Ethiopia and its adjoining regions. Geoenvironm Disasters 6(1):25. https://doi.org/10.1186/s40677-019-0131-y
Letamo A, Kavitha B, Tezeswi TP (2023) Seismicity pattern of African regions from 1964–2022: b-value and energy mapping approach. Geomatics Nat Hazards Risk 14(1):25. https://doi.org/10.1080/19475705.2023.2197104
Lolli B, Gasperini P, Vannucci G (2014) Empirical conversion between teleseismic magnitudes (mb and Ms) and moment magnitude (Mw) at the Global, Euro-Mediterranean and Italian scale. Geophys J Int 199(2):805–828. https://doi.org/10.1093/gji/ggu264
Medvedev S (2016) Understanding lithospheric stresses: Systematic analysis of controlling mechanisms with applications to the African Plate. Geophys J Int 207(1):393–413. https://doi.org/10.1093/gji/ggw241
Mobarki M, Talbi A (2022) Spatio-temporal analysis of main seismic hazard parameters in the Ibero-Maghreb region using an Mw-homogenized catalog. Acta Geophys 70(3):979–1001. https://doi.org/10.1007/s11600-022-00768-w
Muller C, Jokat W (2000) Seismic evidence for volcanic activity discovered in central Arctic. Eos Trans Am Geophys Union 81(24):265–269
Rajaonarison TA, Stamps DS, Naliboff J (2021) Role of lithospheric buoyancy forces in driving deformation in East Africa from 3D geodynamic modeling. Geophys Res Lett 48(6):1–10. https://doi.org/10.1029/2020GL090483
Sanchez JJ, Mccausland W, Clifford T, Sanchez JJ (1995) Spatial variations in the frequencymagnitude distribution of earthquakes at Mount Pinatubo Volcano
Schorlemmer D, Wiemer S, Wyss M (2005) Variations in earthquake-size distribution across different stress regimes. Nature 437(7058):539–542
Scordilis EM (2006) Empirical global relations converting MS and mb to moment magnitude. J Seismolog 10(2):225–236. https://doi.org/10.1007/s10950-006-9012-4
Stamps DS, Flesch LM, Calais E, Ghosh A (2014) Current kinematics and dynamics of Africa and the East African Rift System. J Geophys Res Solid Earth 119(6):5161–5186
Wason HR, Das R, Sharma ML (2012) Magnitude conversion problem using general orthogonal regression. Geophys J Int 190(2):1091–1096. https://doi.org/10.1111/j.1365-246X.2012.05520.x
Weatherill GA, Pagani M, Garcia J (2016) Exploring earthquake databases for the creation of magnitude-homogeneous catalogues: tools for application on a regional and global scale. Geophys J Int 206(3):1652–1676. https://doi.org/10.1093/gji/ggw232
Wiemer S (2001) A software package to analyze seismicity: ZMAP. Seismol Res Lett 72(3):373–382. https://doi.org/10.1785/gssrl.72.3.373
Williams JN, Wedmore LNJ, Fagereng Å, Werner MJ, Mdala H, Shillington DJ, Scholz CA, Kolawole F, Wright LJM, Biggs J, Dulanya Z, Mphepo F, Chindandali P (2022) Geologic and geodetic constraints on the magnitude and frequency of earthquakes along Malawi's active faults: the Malawi Seismogenic Source Model (MSSM). Nat Hazard 22(11):3607–3639. https://doi.org/10.5194/nhess-22-3607-2022
Yang Z, Chen WP (2010) Earthquakes along the East African Rift System: a multiscale, system-wide perspective. J Geophys Res Solid Earth 115(12):1–31. https://doi.org/10.1029/2009JB006779

Publisher's Note

Springer Nature remains neutral with regard to jurisdictional claims in published maps and institutional affiliations.